ISBN: 978-3-95450-250-9 ISSN: 2673-5520 doi:10.18429/JACoW-MEDSI2023-THOBM04

DEVELOPMENT OF A MIRROR CHAMBER FOR SHINE PROJECT

F. Liu†, T. Wu, S. He, H. Yuan, X. Zhang, Z. Wang, W. Li
Center for Transformative Science, ShanghaiTech University, Shanghai, China
L. Zhang, J. Chen, W. Zhu
Shanghai Advanced Research Institute, CAS, Shanghai, China

Abstract

A 5-DOF mirror chamber test system was developed to adjust offset mirror or distribution mirror for the SHINE project. Two linear guides were used for horizontal translation and coarse pitch adjustments. Three vertical gearboxes were used for height, roll and yaw adjustments. In the vacuum, a fine flexure structure was engineered for the fine pitch adjustment with a piezo actuator. To prevent the cooling vibrations, the cooling module was separately fixed and the heat from the mirror was conducted by Ga/In to the cooling blade. Pitch angular vibration were measured by several equipment under different conditions. Results showed that the pitch angular vibration was below 40 nrad above 1 Hz without active vibration control, and below 10 nrad with active vibration isolation system.

INTRODUCTION

Shanghai HIgh repetitioN rate XFEL and Extreme light facility (SHINE) started the ground breaking on 27th April, 2018. The whole facility is 3.1 km long installed in the tunnels about 29 meters underground. The whole facility was shown in Fig. 1. The first 1.5 kms were for the linac to accelerate the electron bunches up to 8 GeV, and generate X rays in the range between 0.4~25 keV within 3 beamlines. In the Near Experimental Hall (NEH) and Far Experimental Hall (FEH), 10 endstations were built in the first phase. As shown in Fig. 1, there was highway lying along the facility, and a river passing across the tunnel between Shaft 3 and Shaft 4, and a subway Line 13 running right above the tunnel between Shaft 4 and Shaft 5. To investigate the vibration transfer between the ground to the optics, a mirror chamber system was developed according to the requirements of M1 adjustments.

MIRROR CHAMBER SETUP

According to the requirements for the M1 adjustments, the specifications were listed in Table 1 and the schematic of the mirror chamber was shown in Fig. 2. The X translation was used to move the mirror in and out of the beam when necessary, the Z translation was intended to change the stripe of the mirror, however, considering the ground settlement of the tunnel, 100 mm adjustment range was designed. To make a stable and reliable chamber system, most of the adjustments were put outside the vacuum, and the vacuum chamber was supported separately.

The whole mirror chamber system was shown in Fig. 3, the base was made of two granites, in between were four air bearings, and two linear translations were installed in the two ends. When the translation move in the same direction, horizontal movement was realized, when they move in opposite directions, a pitch angle would appear (detailed in Fig. 4) [1]. For the vertical translation and the roll and yaw adjustment, since no fine adjustments were necessary, ordinary gearboxes were employed, however, the stiffness in the radial directions were carefully designed to meet pitch angle stabilities. And the contacts of the three kinematic supports were also optimized for better stability issues. To minimize the influence by water cooling, the mirror was cooled by a copper blade inserted in an Indium Galium eutectic bath on the mirror, and the cooling tubes were fixed to a separate support decoupled to the mirror holder as shown in Fig. 5. Considering the vertical translation when exchanging the stripes on the mirror, the water cooling movement was coupled to the vertical translation of the mirror holder by connecting the two gearboxes with a shaft.

Figure 1: Topview of the SHINE facility.

† liufang@shanghaitech.edu.cn

ISBN: 978-3-95450-250-9 ISSN: 2673-5520 doi:10.18429/JACoW-MEDSI2023-THOBM04

Table 1: Specifications of the Mirror Chamber System

Axis	Range	Resolution
Mirror X translation (in/out beam)	± 40 mm	2 µm
Mirror Z translation (High adjustment)	± 50 mm	5 µm
Pitch (coarse)	± 8 mrad	10 µrad
Pitch (fine)	± 70 µrad	5 nrad
Roll	± 1°	10 µrad**
Yaw	± 200 µrad	10 µrad
Z translation of Chamber (manual)	80 mm	0.1 mm
X translation of Chamber (manual)	± 30 mm	0.1 mm

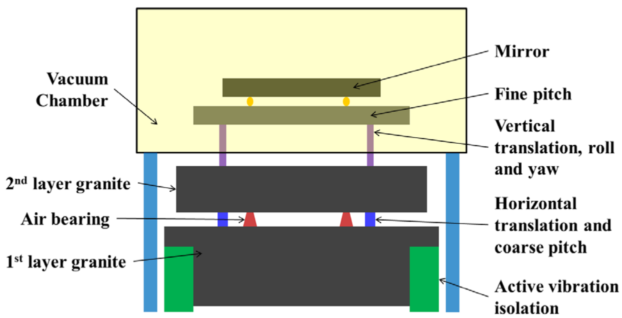

Figure 2: Schematic of the mirror chamber system.

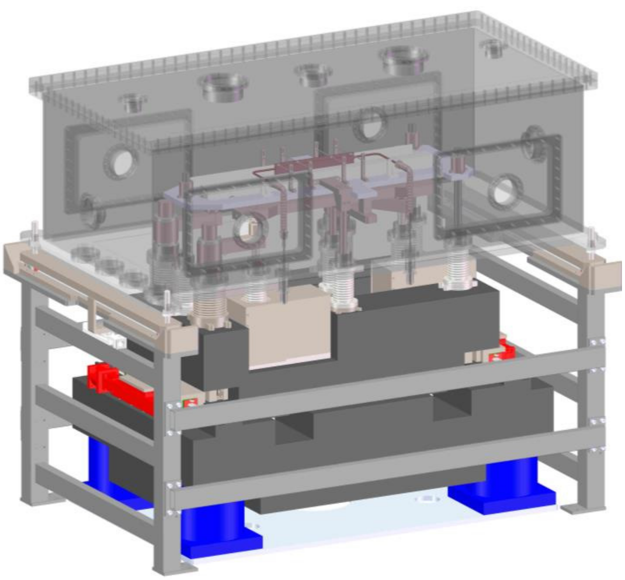

Figure 3: 3D model of the mirror chamber system.

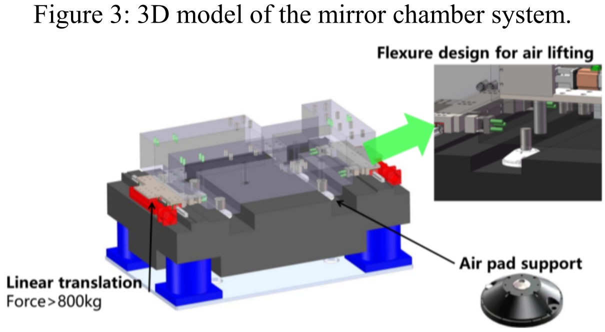

Figure 4: Model of coarse pitch and X-translation with air pad support.

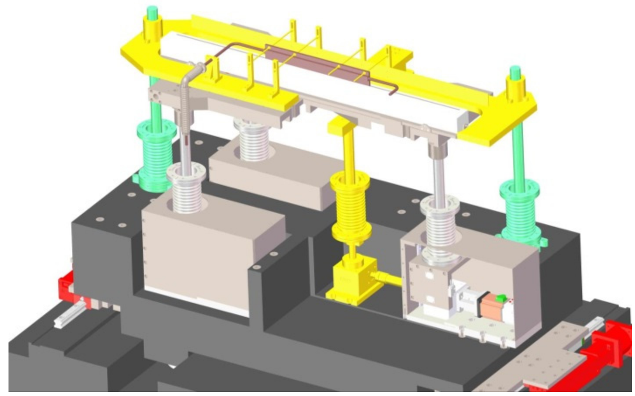

Figure 5: Mirror cooling was decoupled to the cooling blade, while the movement of the water cooling was coupled to the vertical translation of the mirror.

An active vibration isolation system (STACIS-III, TMC) using piezo compensation was chosen to isolate the ground vibrations, and hopefully to keep the same position relative to the ground below 2 Hz.

MEASUREMENT AND DISCUSSION

The real mirror chamber system without vacuum chamber was shown in Fig. 6. The movement of the coarse pitch and translation were measured by 5529A Dynamic Calibration System (Keysight) [2], the resolution of the fine pitch was measured by IDS3010 (attocube GmbH) [3], and the pitch angular vibrations of the mirror were measured in three ways as demonstrated in Fig. 7. The absolute angular velocity of pitch was measured by using two geophones (941B) [4] glued to the mirror dummy made of aluminium 800mm in distance as labelled in V1 and V2 in Fig. 7. The relative angle between the ground and the mirror was measure by 5529A, and the relative angle between the upper granite and mirror was measured by IDS3010.

As shown from Fig. 8 to Fig. 10, the resolution of X translation was better than 167 nm, coarse pitch angular resolution was 1.5 µrad and the range was over ±10 mrad. The fine pitch resolution was 5 nrad shown in Fig. 11.

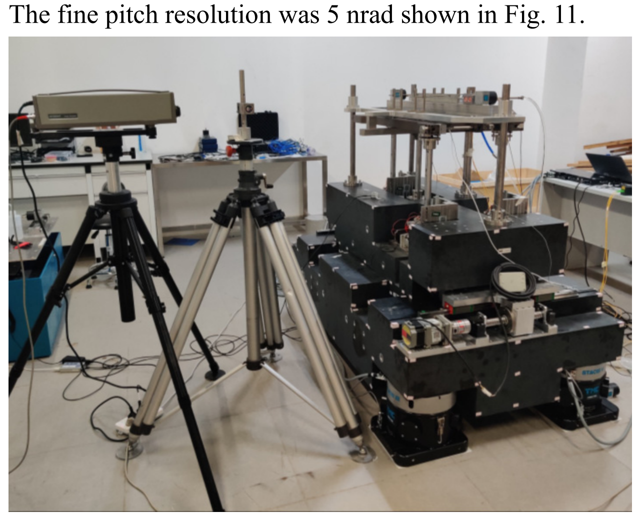

Figure 6: Mirror chamber system and the measurement set up.

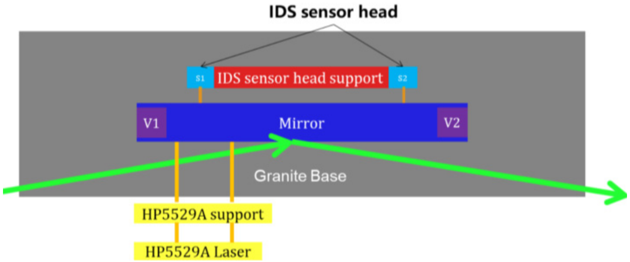

Figure 7: Measurement set up for pitch angle of the mirror.

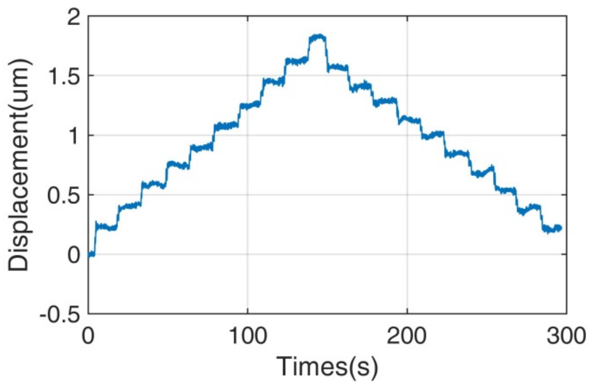

Figure 8: X translation was tested with each step of 167 nm when airpads were pressurized.

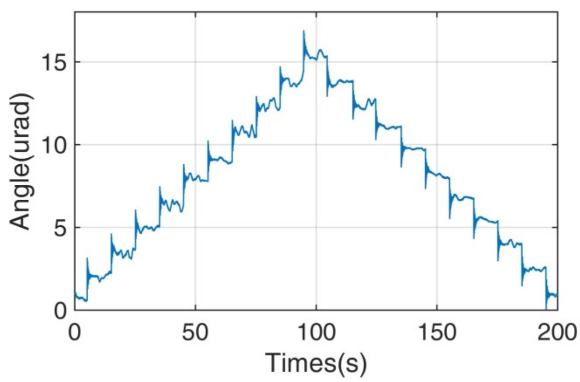

Figure 9: Coarse pitch was tested with each step of 1.5 µrad when airpads were pressurized.

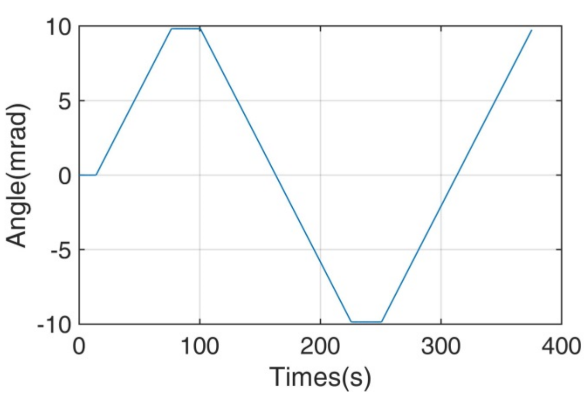

Figure 10: Coarse pitch range was moved from −10 mrad to 10 mrad.

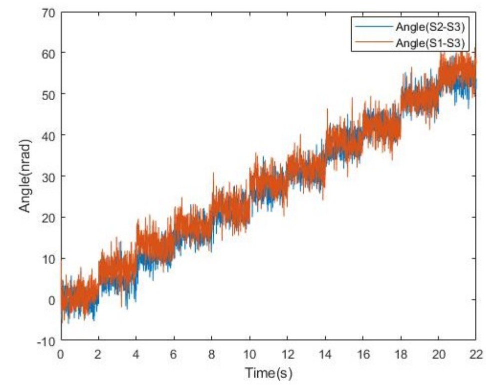

Figure 11: Fine pitch was tested with each step of 2 nm by the piezo, resulting about a 5 nrad resolution.

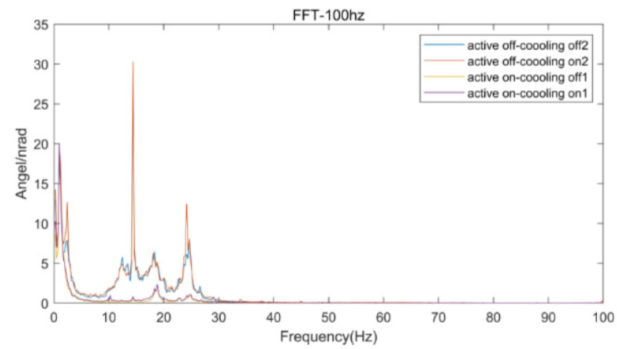

Figure 12: Absolute pitch vibration comparison with and without cooling when active vibration isolation system on and off in spectrum.

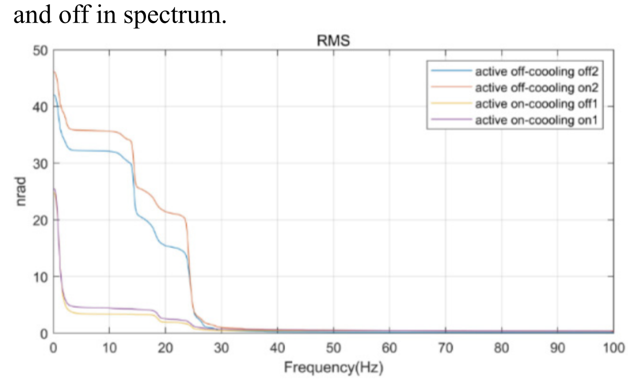

Figure 13: Absolute pitch vibration comparison with and without cooling when active vibration isolation system on and off in statistics.

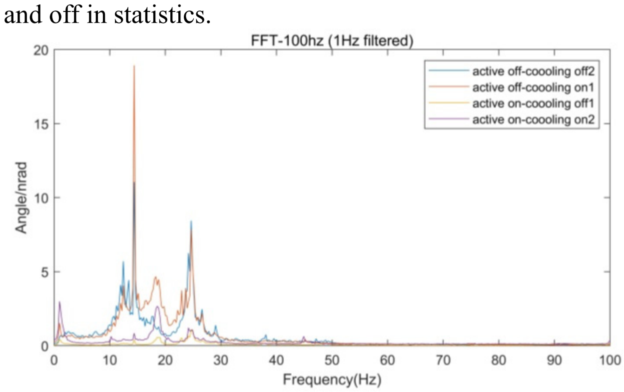

Figure 14: Pitch vibration comparison between mirror and granite with and without cooling when active vibration isolation system on and off in spectrum.

ISBN: 978-3-95450-250-9 ISSN: 2673-5520 doi:10.18429/JACoW-MEDSI2023-THOBM04

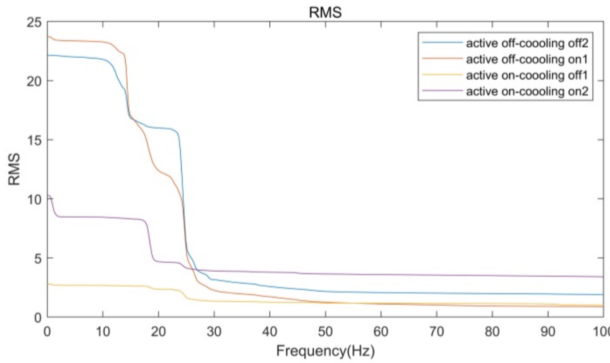

Figure 15: Pitch vibration comparison between mirror and granite with and without cooling when active vibration isolation system on and off in statistics.

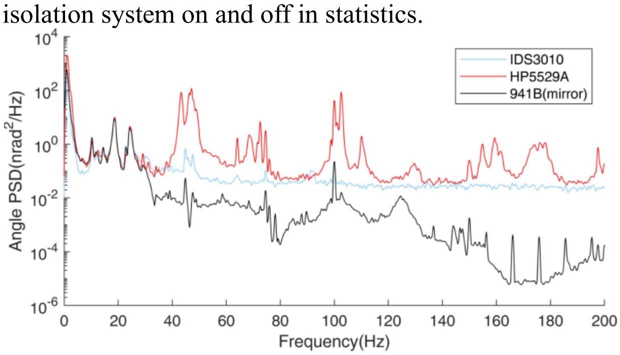

Figure 16: Spectrum comparison of pitch angle with different measurements when active vibration isolation was enabled and water cooling was functioning.

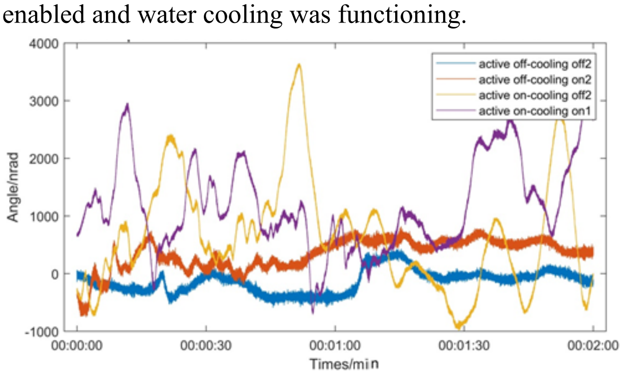

Figure 17: Waveform of pitch angle comparison between mirror and ground with and without cooling when active vibration isolation system on and off.

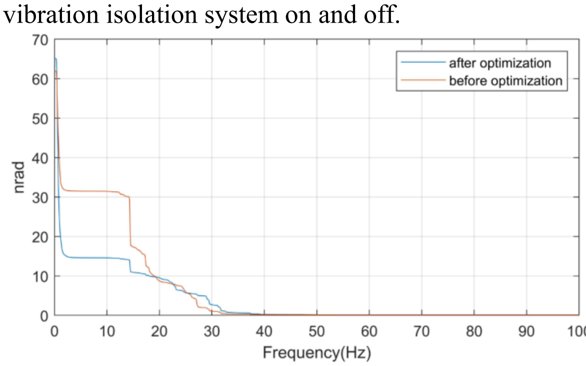

Figure 18: Comparison of stabilities with the optimization of the joints connecting to the pillars of the gearboxes.

Figure 12 to Fig. 15 showed the spectrum as well as the RMS vibrations measured by geophones and IDS with a 1Hz high pass filter applied to the data when the airpads were seated on the granite. Figures 12 and 13 showed that the absolute pitch vibration was about 40 nrad without active vibration isolation, the relative pitch angular vibration was about 25 nrad between mirror and the granite. Most of the vibration spectrums were below 30 Hz. When the active vibration isolation was enabled, the pitch vibration was below 10 nrad in both measurements. Figure 15 also indicated that the effect of water cooling was less than 8 nrad (water flow was 4 L/min) by comparing the data when active vibration isolation was enabled. Figure 16 showed the spectrum of the three measurements comparison when active vibration isolation was enabled and water cooling was on. By comparing the spectrums, it showed that in the range of 2-30 Hz, the spectrum were consistent by all three methods, which was also the main spectrums of the vibration. For HP5529A, spectrum above 40 Hz was higher than the other two methods, which was due to the vibration caused by the support itself. For the IDS, spectrums above 50 Hz were about the same, it was explained that this was the signal noise of the instrument. Figure 17 was the waveforms of the pitch angles in 2 minutes. When active vibration isolation was disabled, the width of the waveform were bigger than the width when active vibration isolation was active, which indicated that the active vibration isolation did improve the high frequency vibrations. However, there were another random slow motions up to 5 μrad were observed. The reason was not yet clear. Figure 18 indicated that the joints connections were also important, by optimization, stability was improved from 30 nrad to 15 nrad.

CONCLUSION

A 5-DOF high heat-load and high stability mirror chamber test system was developed to demonstrate the stability performance in the SHINE environment. Results showed that the stability was under 40 nrad with water cooling. By decoupling the cooling blade and the support, the effect by water cooling could be minimized to 8 nrad. By isolating the ground vibration with active vibration isolation system, the pitch angle vibration reduced to less than 10 nrad. By optimizing the joints of connecting to the pillars, vibration could be further improved.

REFERENCES

[1] F. Liu, Z. Liu and Y. Chen, “A two-dimensional high stability adjustment mechanism”, National Intellectual Property Bureau of China, 202111035778.2, Jul. 25, 2023.

[2] `https://www.keysight.com/us/en/product/5529A/dynamic-calibration-system.html`

[3] `https://www.attocube.com/en/products/laser-displacement-sensor/displacement-measuring-interferometer`

[4] `http://www.topreascend.com/tprs-Products-7397129/`